

Magnetic Microscopy: seeing is believing

An introduction to magnetic image simulation using:

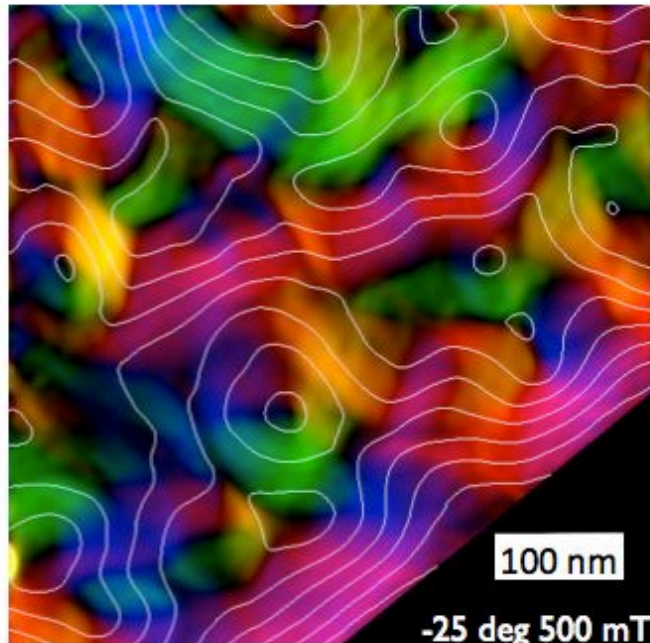


Why the need for forward modelling?

The primary goal of magnetic microscopy is to image the magnetisation state of your sample. However, most magnetic microscopy methods measure quantities that are only indirectly related to the underlying magnetic moment distribution.

Interpretation of the signal is complicated by:

- Sample geometry
- Sample heterogeneity
- Instrumental resolution/noise/artefacts
- Non-uniqueness of the inverse problem

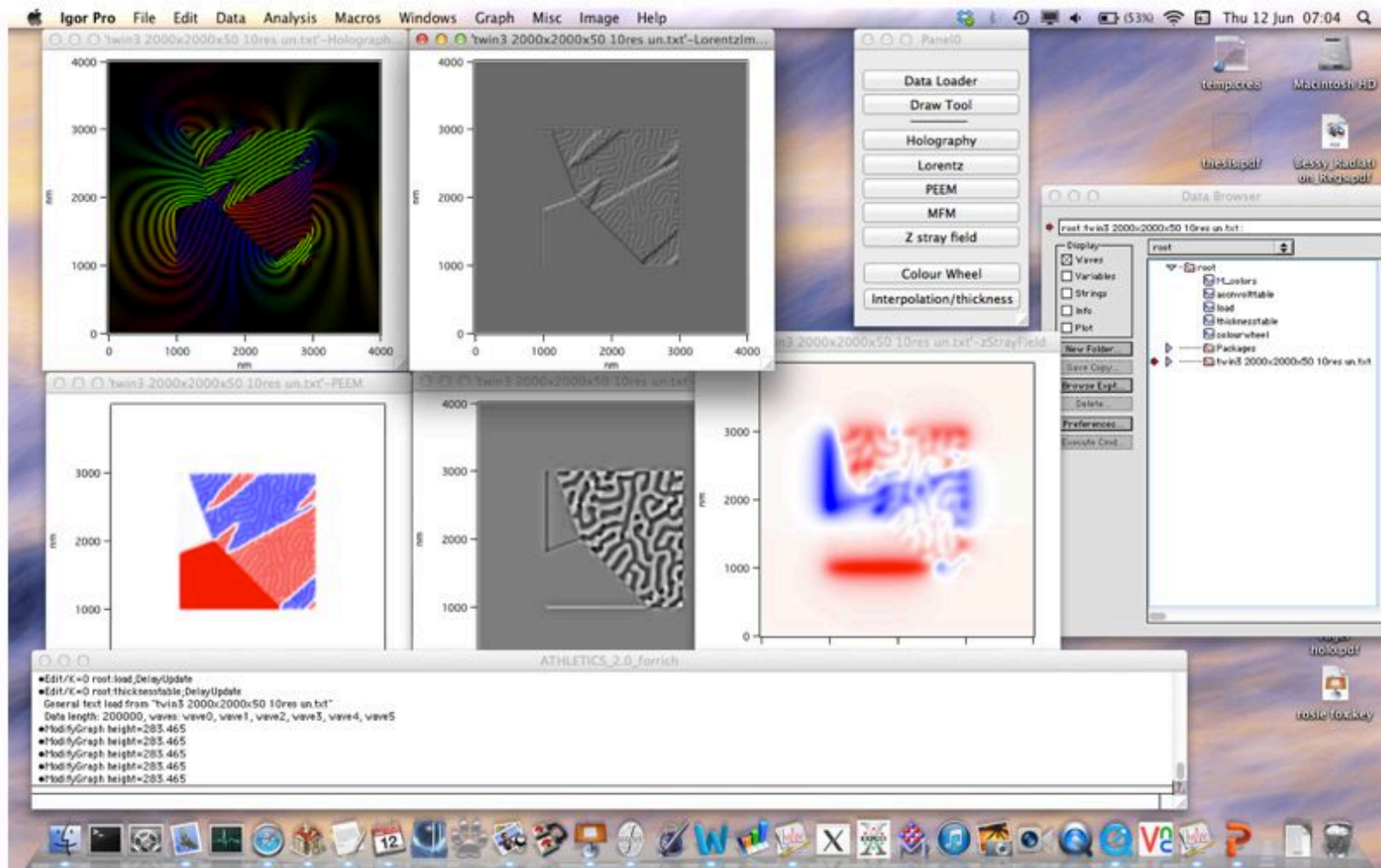


What exactly are we seeing here?

Holography measures electron phase shift, which is determined by integrated magnetic induction along the electron beam path, which is sensitive to the magnetisation of the sample plus the internal demagnetising field plus the external stray field all modulated by variations in sample thickness, internal composition, the presence of the sample edge...

ATHLETICS

A Tremendous Holography and Lorentz Image Creation Simulator (blame James...)



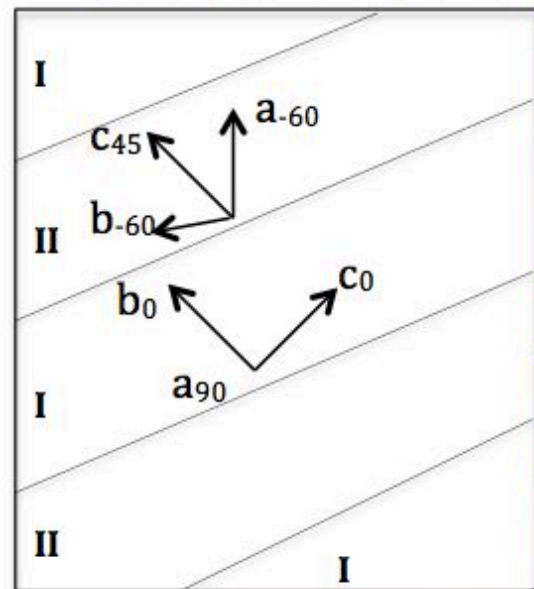
James F.J. Bryson, Takeshi Kasama, Rafal E. Dunin-Borkowski & Richard J. Harrison (2012): Ferrimagnetic/ferroelastic domain interactions in magnetite below the Verwey transition: Part II. Micromagnetic and image simulations. *Phase Transitions: A Multinational Journal*, DOI:10.1080/01411594.2012.695372

Theory (holography)

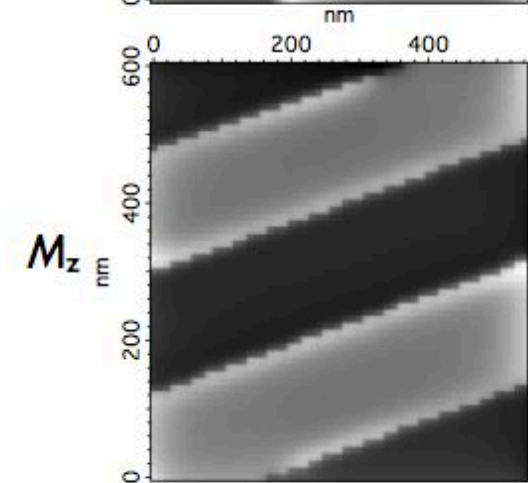
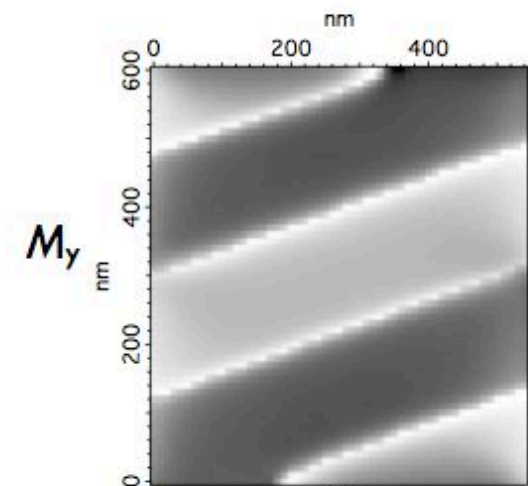
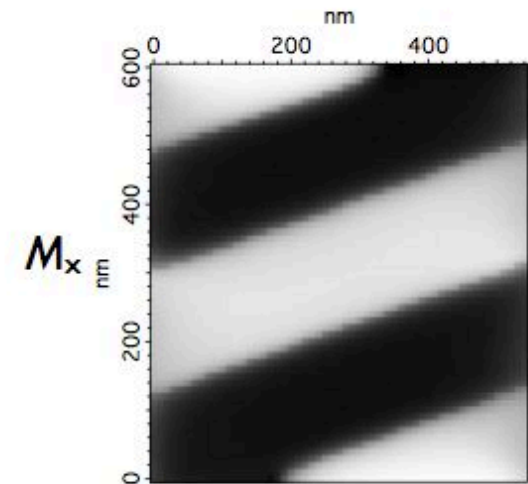
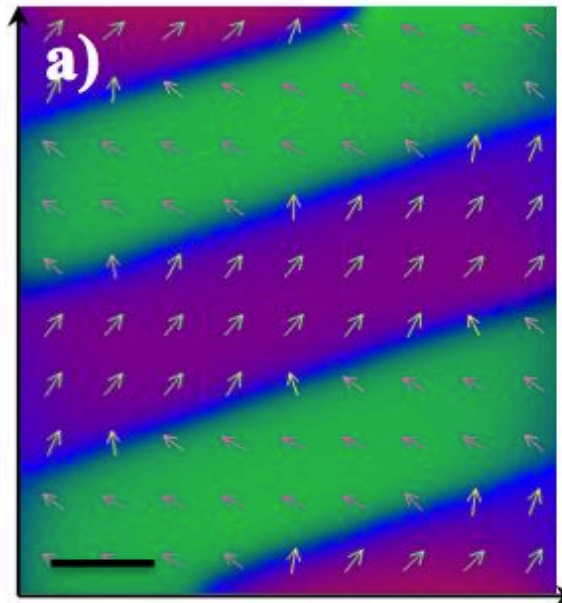
Input to the image simulation is in the form of three 3D matrices, M_x , M_y , M_z , describing the x, y and z, components of the magnetisation unit vectors.

The M_x , M_y and M_z matrices can either be the result of a micromagnetic simulation, or they can be generated by hand to test a specific hypothesis.

e.g. Magnetite below the Verwey transition containing twins with differently oriented magnetocrystalline easy axes.



Equilibrium domain structure obtained by micromagnetic simulation.

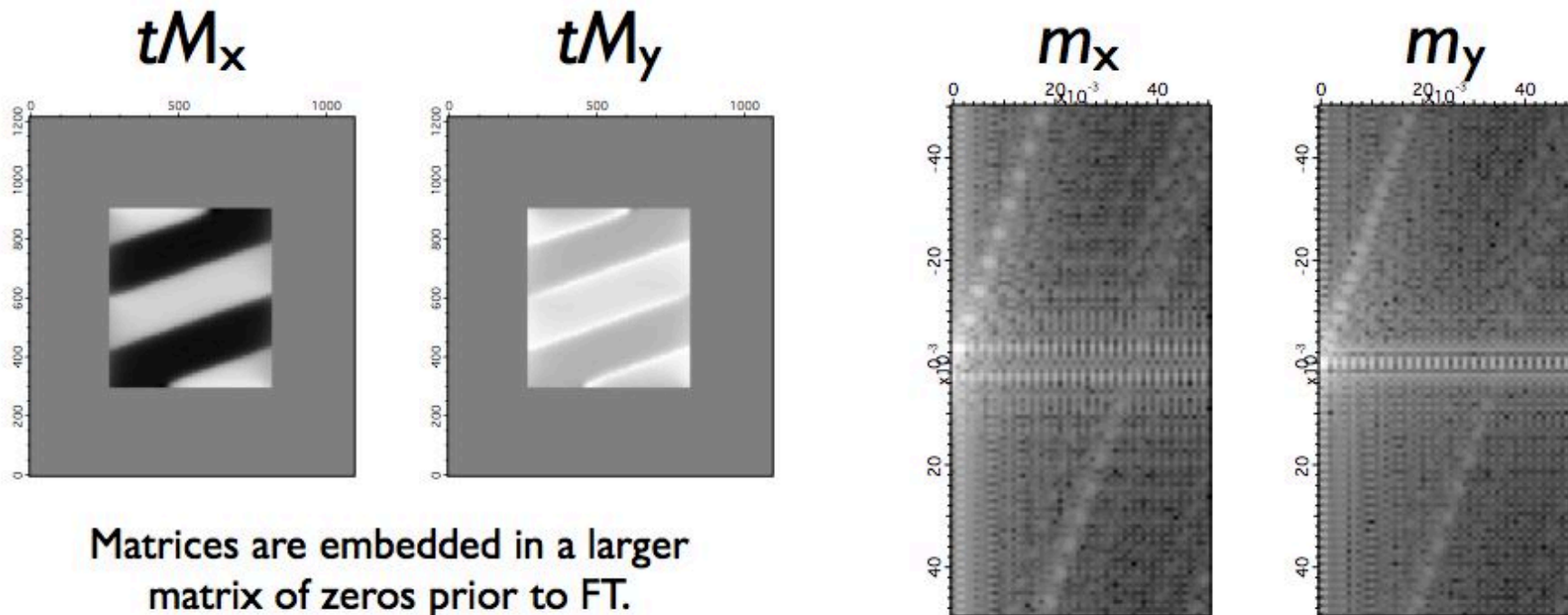


Theory (holography)

In holography and Lorentz microscopy, the measured phase shift only depends on the in-plane (x, y) components of magnetisation. M_x and M_y matrices are averaged along the z direction. These matrices are then multiplied by the sample thickness, t (in nm), and Fourier transformed:

$$\mathcal{F}(t\mathbf{M}_x(x, y)) = \mathbf{m}_x(k_x, k_y)$$

$$\mathcal{F}(t\mathbf{M}_y(x, y)) = \mathbf{m}_y(k_x, k_y)$$



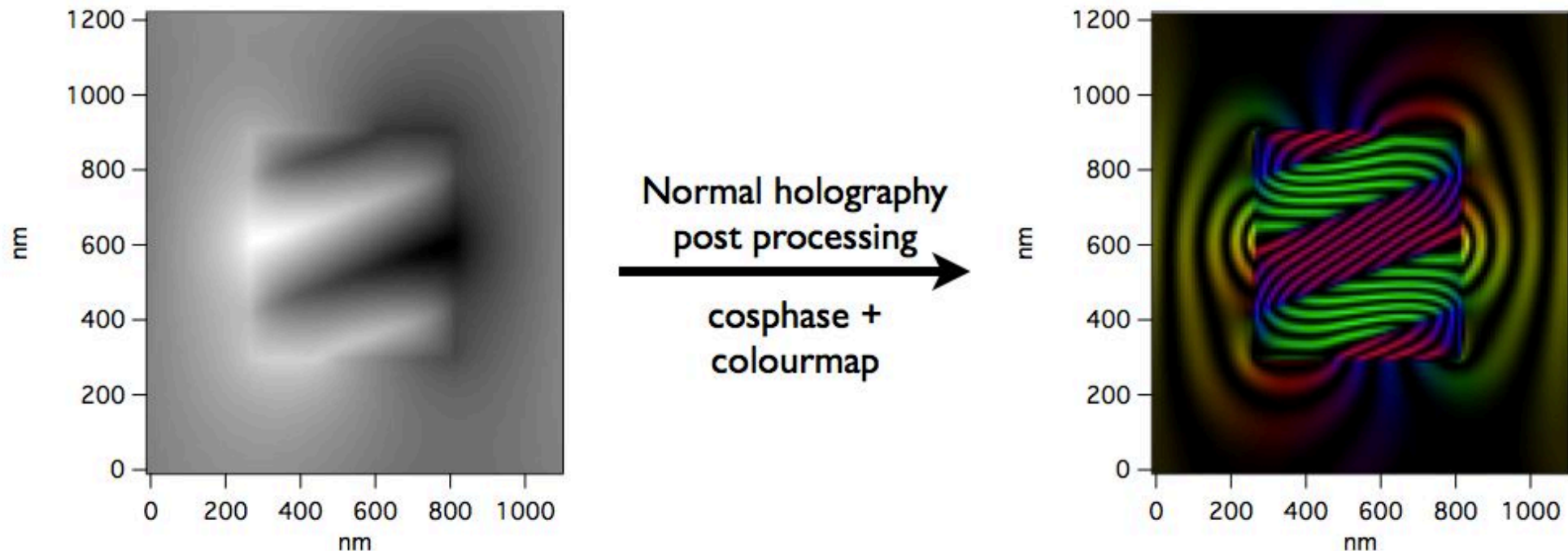
Matrices are embedded in a larger matrix of zeros prior to FT.

Theory (holography)

In Fourier space, the phase shift, $\phi(\mathbf{k})$, is given by (Beleggia and Zhu 2003):

$$\varphi(\mathbf{k}) = \frac{i\pi B_0}{\phi_0} \frac{(k_y \mathbf{m}_x - k_x \mathbf{m}_y)}{k_x^2 + k_y^2}$$

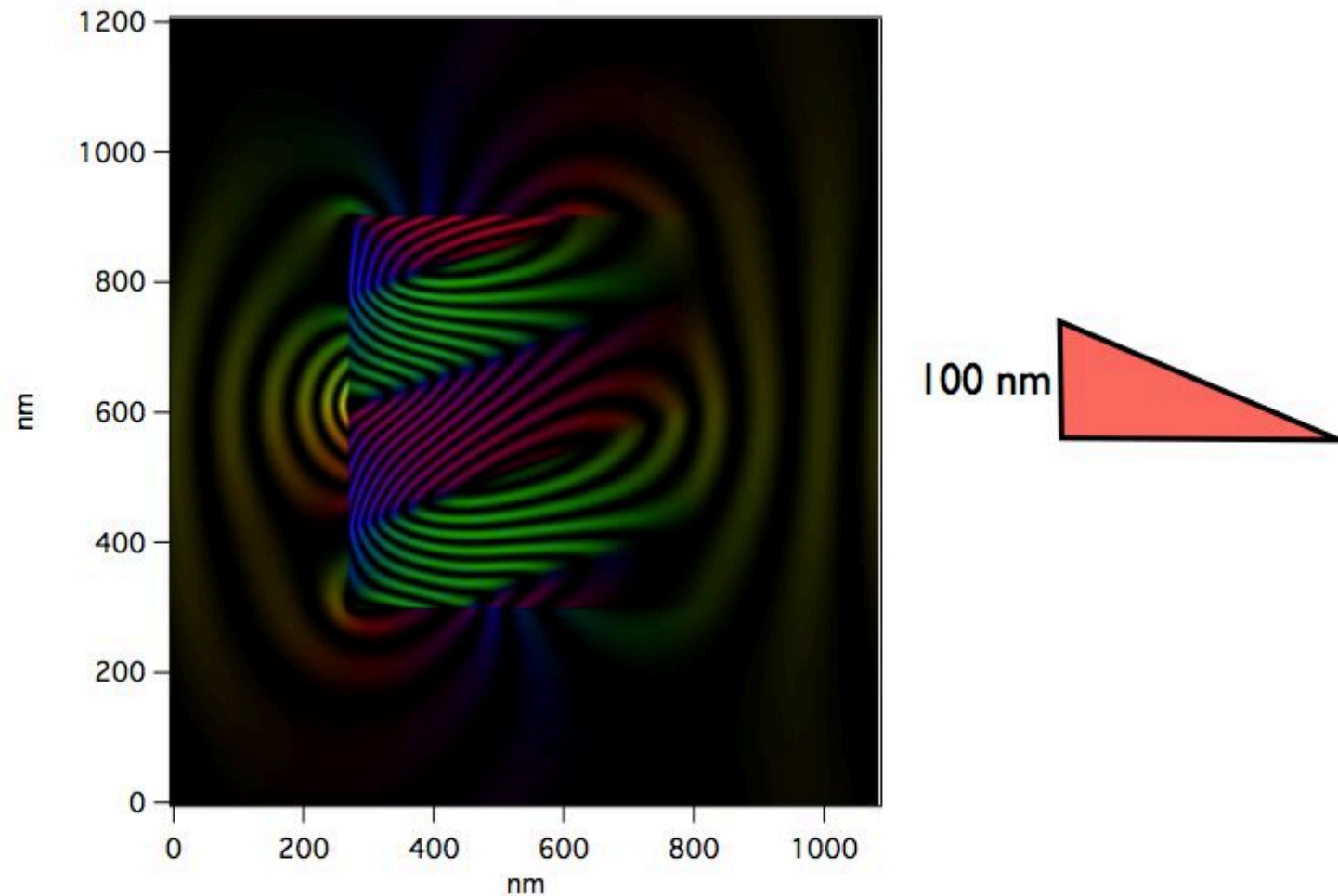
where $\phi_0 = 2067 \text{ Tnm}^2$, $B_0 = \mu_0 M_s$ and k_x and k_y are the reciprocal vectors in Fourier space. Inverse Fourier transform then leads to the phase shift in real space.



Theory (holography)

Additional effects due to mean inner potential and/or thickness variations can be taken into account. Bilinear interpolation of the magnetisation can be used to produce higher resolution results (improves sampling of reciprocal space).

e.g. modelling the effect of a thickness ramp at sample edge
4 x interpolation



Theory (Lorentz microscopy)

Lorentz contrast images are generated by passing the phase map through the TEM contrast transfer function. First, a complex exit wave, $F(x,y)$, is created:

$$F(x, y) = e^{i\varphi(x,y)}$$

The FFT of the complex exit wave, $F(k)$, is then multiplied by the contrast transfer function, $T(k)$:

$$T(\mathbf{k}) = e^{iB(\mathbf{k})}$$

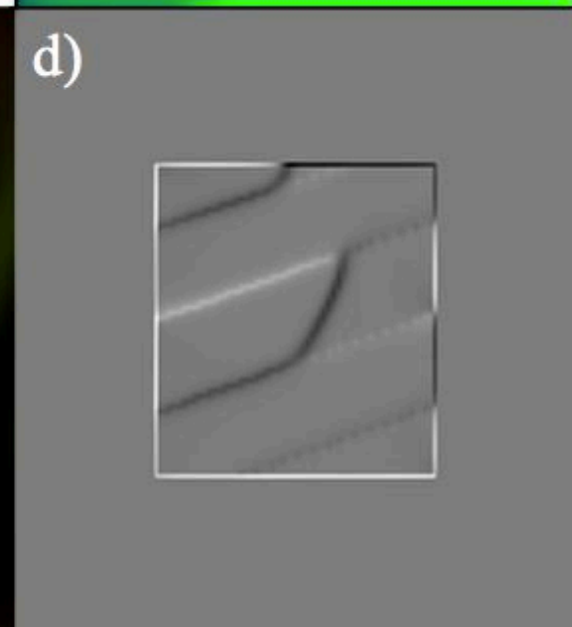
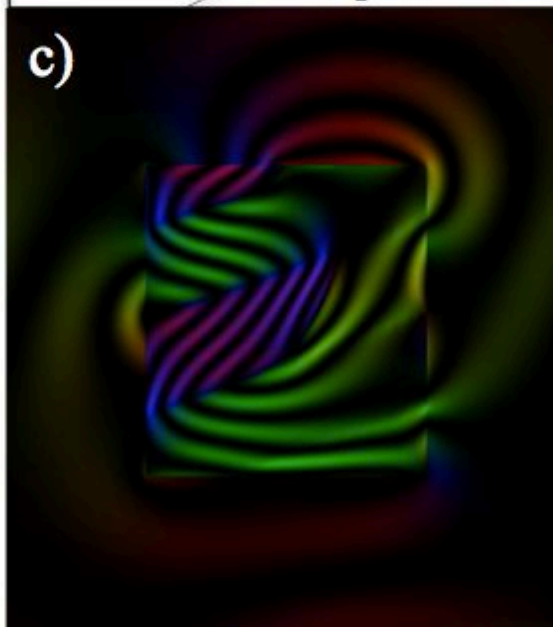
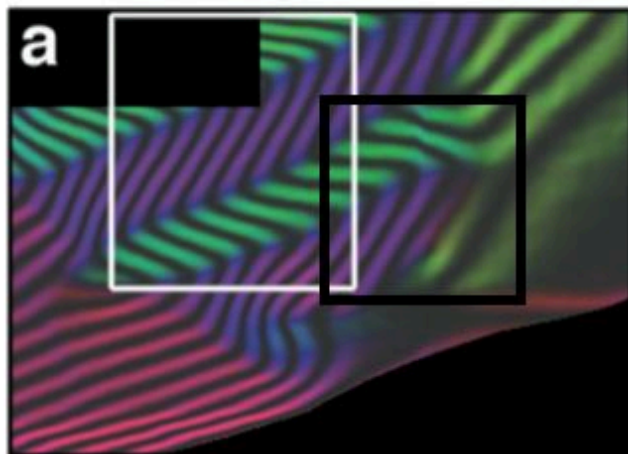
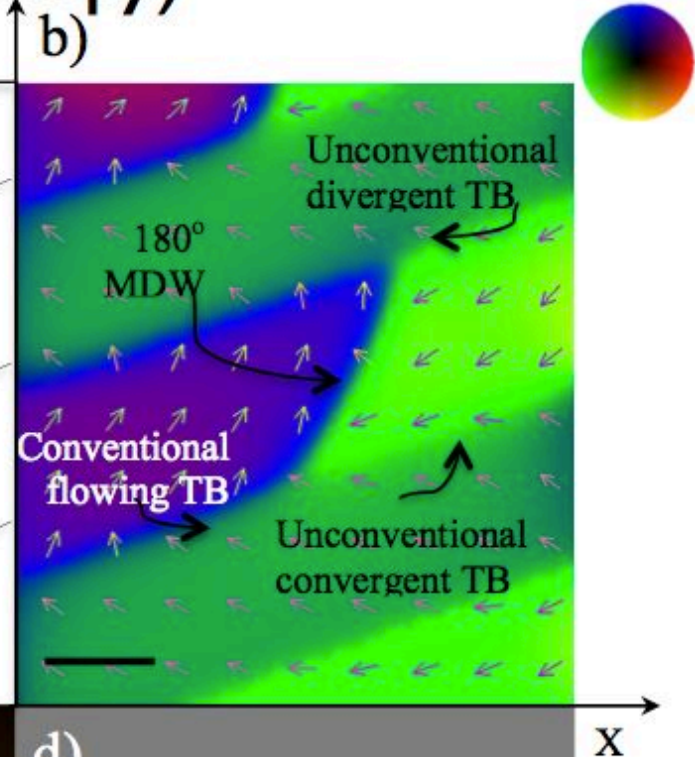
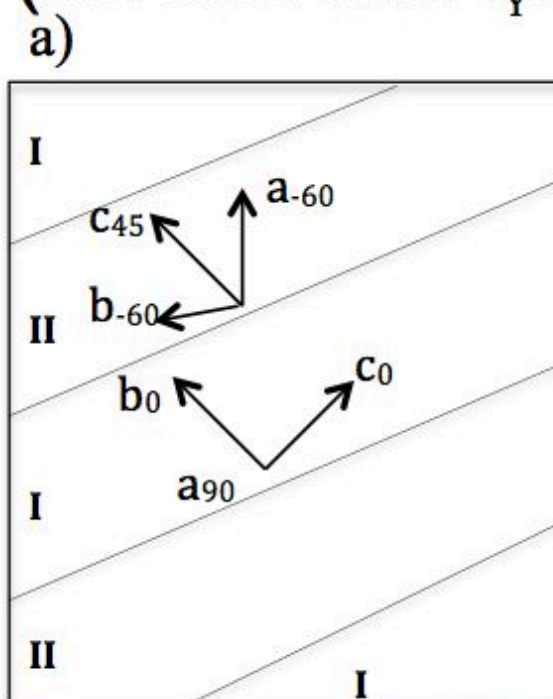
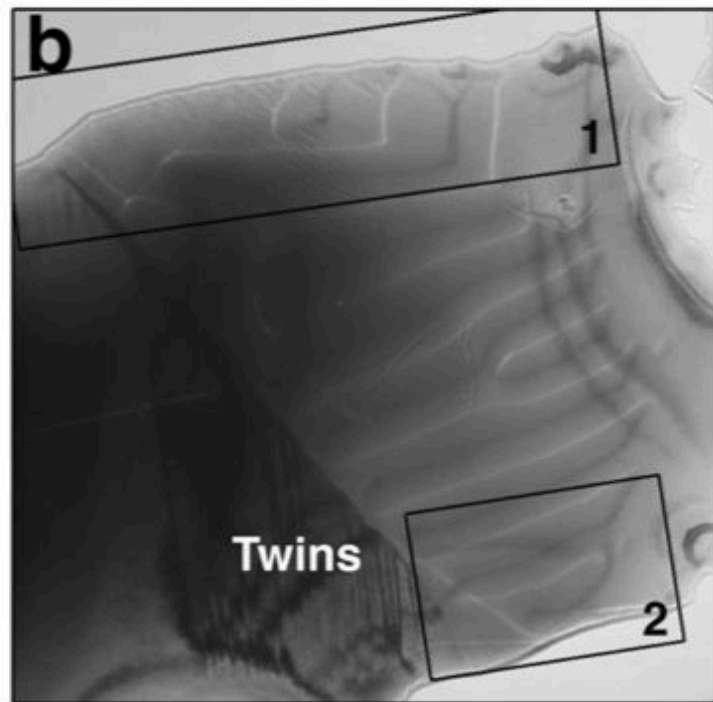
$$I(\mathbf{k}) = F(\mathbf{k})T(\mathbf{k})$$

$$B(\mathbf{k}) = \pi \Delta f \lambda k^2 + \frac{\pi}{2} C_s \lambda^3 k^4$$

where Δf is the defocus value, λ is the wavelength, C_s is the spherical aberration coefficient and $k=(k_x^2+k_y^2)^{1/2}$.

The Lorentz image is then the inverse Fourier transform of $I(k)$.

Theory (Lorentz microscopy)



Theory (Stray field and MFM)

In MFM and stray field calculations, the full 3D matrices can be used in the calculations.

$$\mathcal{F}\left(\frac{B_0 d}{\mu_0} \mathbf{M}_x(x, y, z)\right) = \mathbf{m}_x(k_x, k_y, k_z) \quad \mathcal{F}\left(\frac{B_0 d}{\mu_0} \mathbf{M}_y(x, y, z)\right) = \mathbf{m}_y(k_x, k_y, k_z) \quad \mathcal{F}\left(\frac{B_0 d}{\mu_0} \mathbf{M}_z(x, y, z)\right) = \mathbf{m}_z(k_x, k_y, k_z)$$

where d is the resolution of a pixel in the z direction.

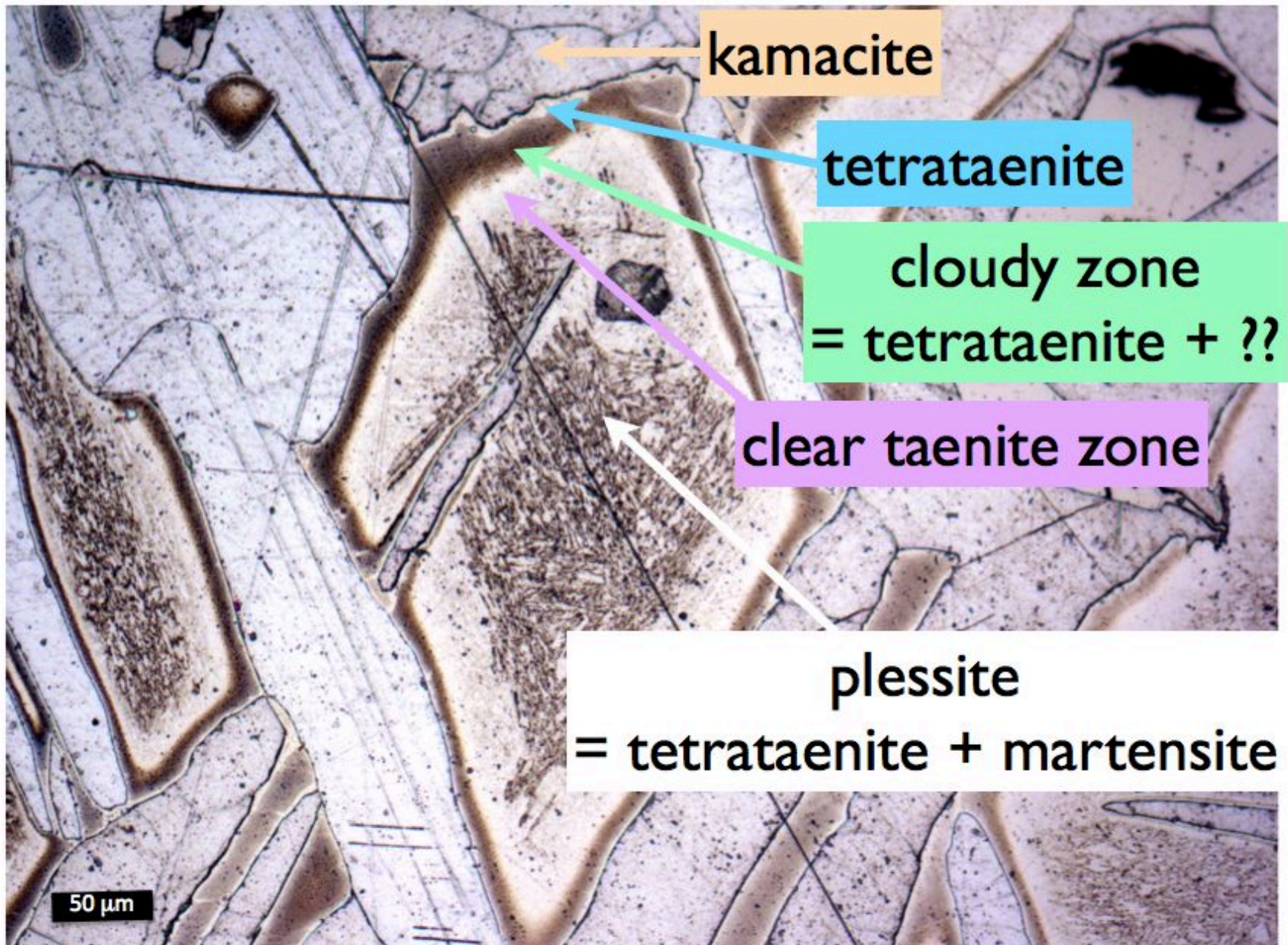
In real-space the stray field can be described as the convolution of the magnetisation with the Green's functions. In Fourier space, this operation is simply a multiplication and the stray field in the out-of-plane direction, b_z , is:

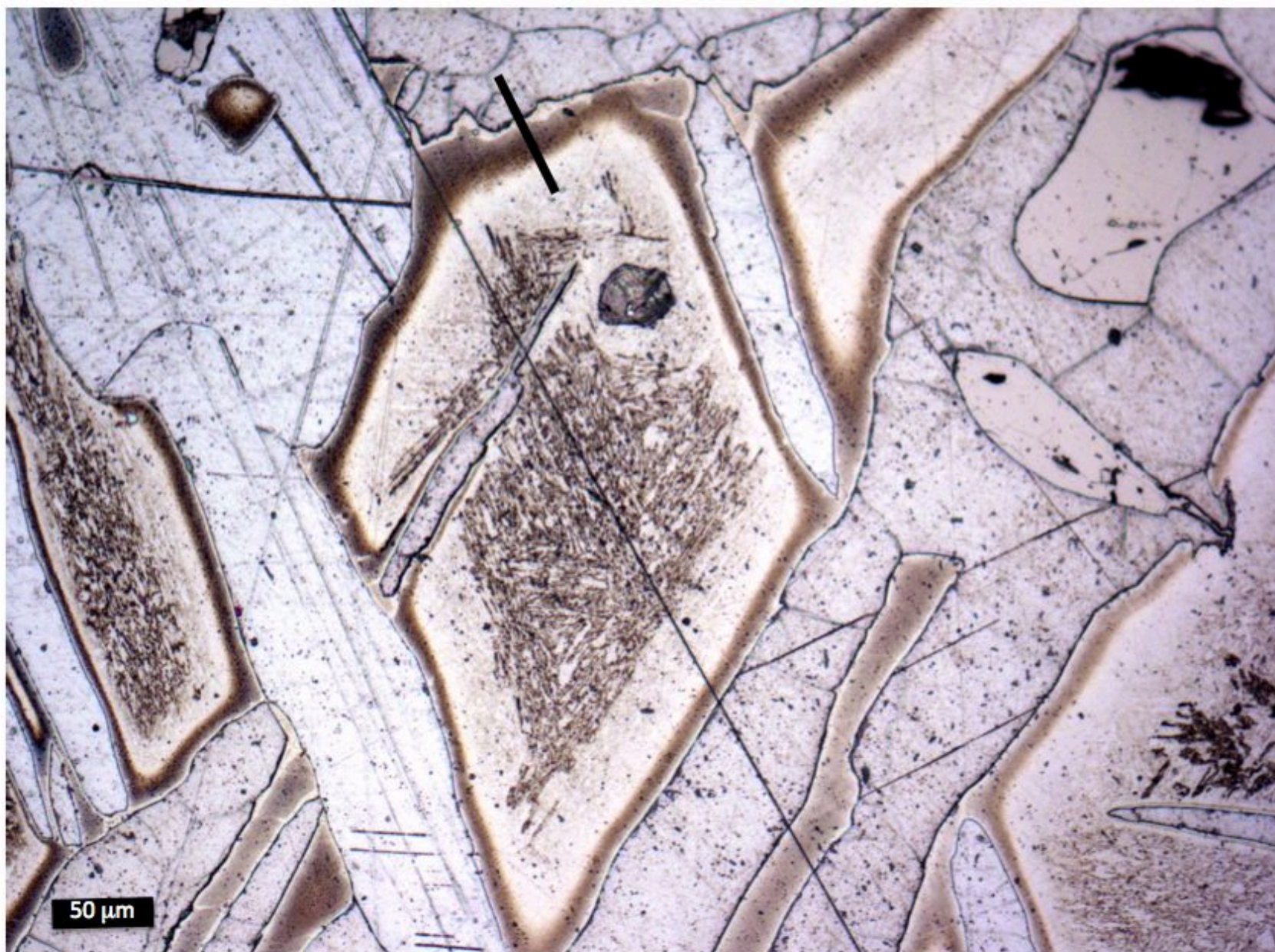
$$b_z(\mathbf{k}) = g_{xz}m_x + g_{yz}m_y + (g_{zz} - g)m_z$$

$$g_{xz} = -\left(\frac{\mu_0}{2}\right)i\kappa_x e^{-h\kappa} \quad g_{yz} = -\left(\frac{\mu_0}{2}\right)i\kappa_y e^{-h\kappa} \quad g_{zz} - g = \left(\frac{\mu_0}{2}\right)i\kappa e^{-h\kappa}$$

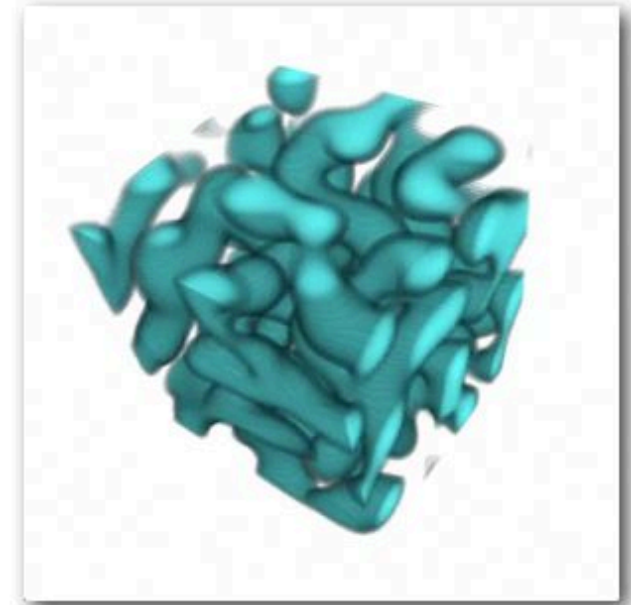
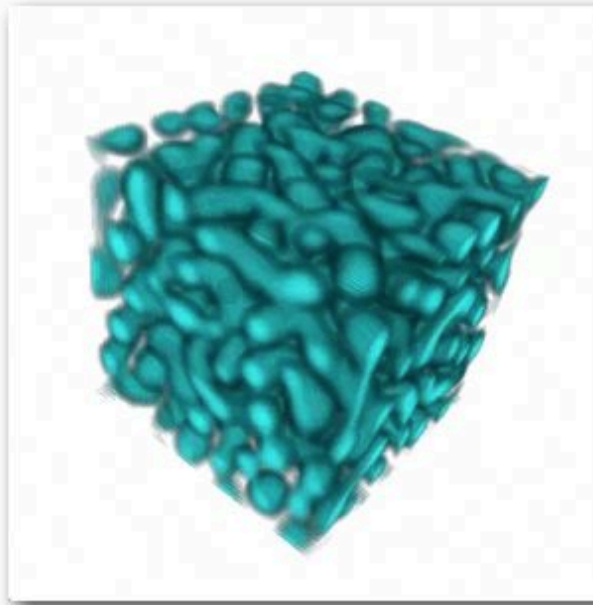
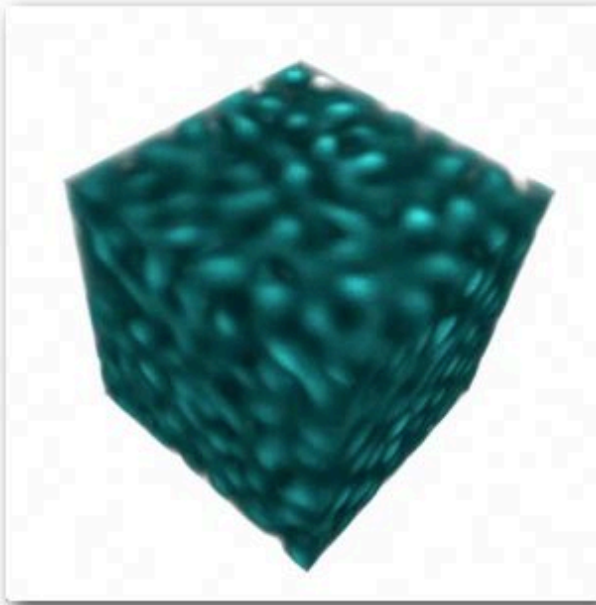
MFM (AC mode) measures the gradient of magnetic force in the z direction, which is proportional to the double derivative of B_z with respect to z . Differentiating along z in Fourier space is achieved by multiplying by k . Hence the inverse Fourier transform of $b_z k^2$ is the signal measured by an MFM.

Example: The Cloudy Zone in Fe-Ni Meteorites



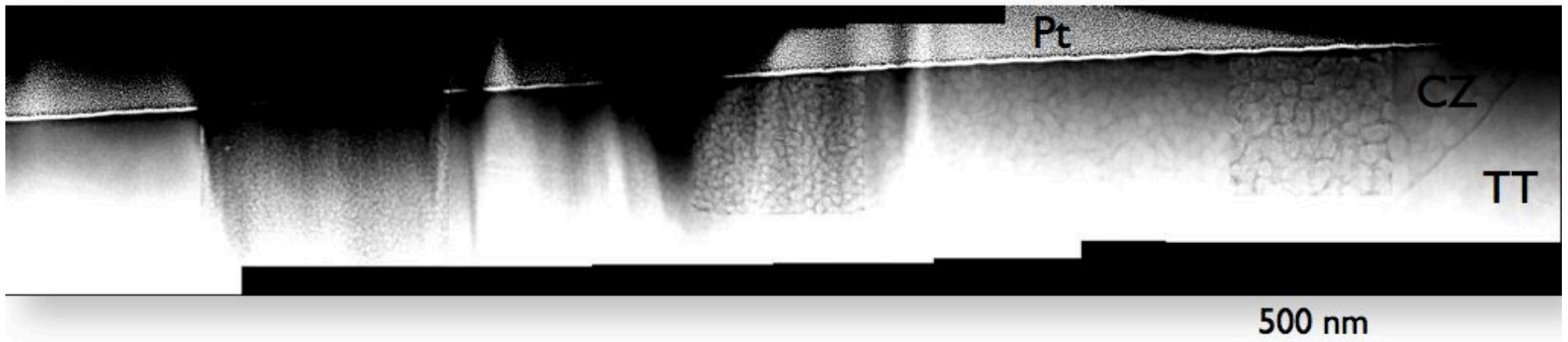


Spinodal Decomposition in the 'Cloudy Zone'

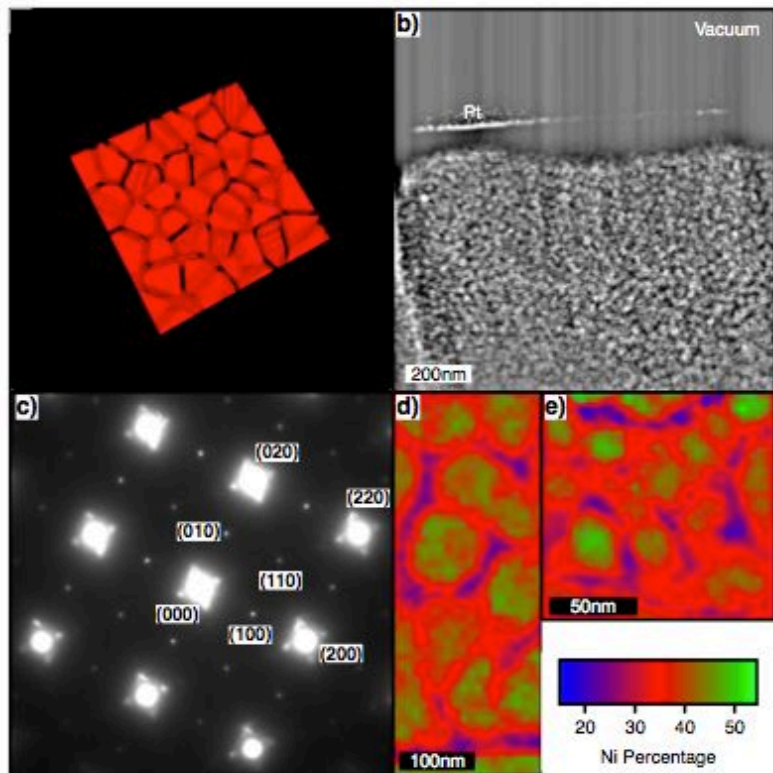


Computer simulations of spinodal development in the fine, medium and coarse cloudy zone

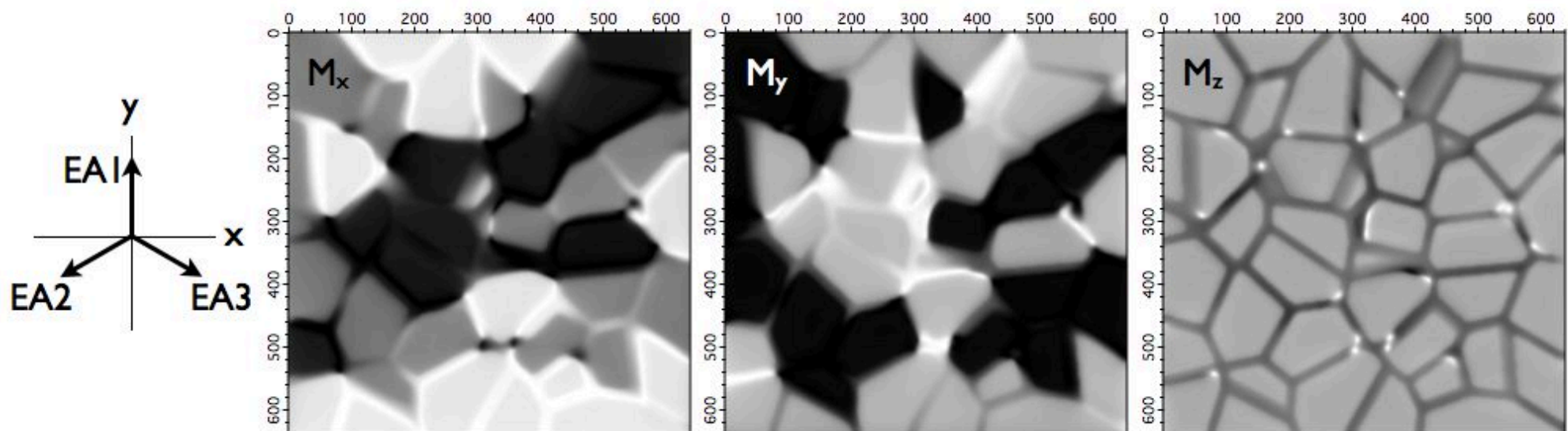
$$\frac{\partial X}{\partial t} = \nabla \cdot \left[\frac{DX_0(1-X_0)}{k_B T} \nabla \left(\frac{df(X)}{dx} - \alpha \nabla^2 X + \mu_{cl} \right) \right]$$



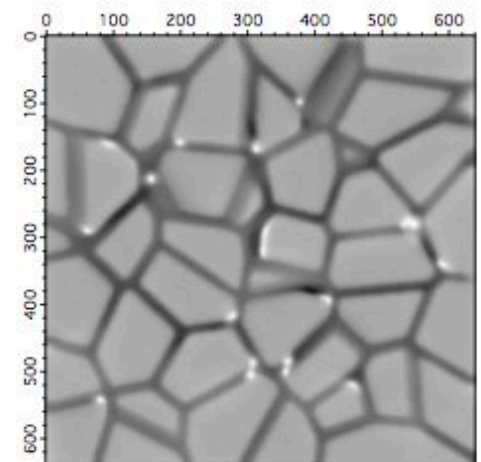
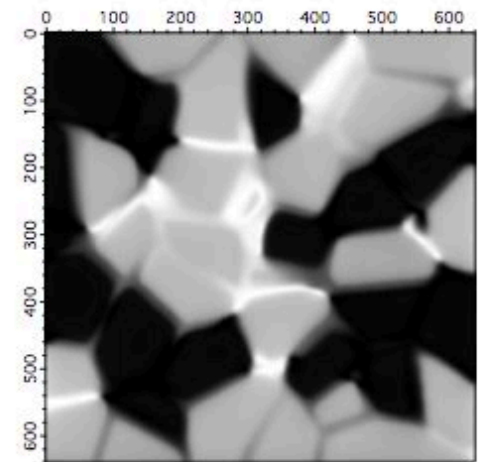
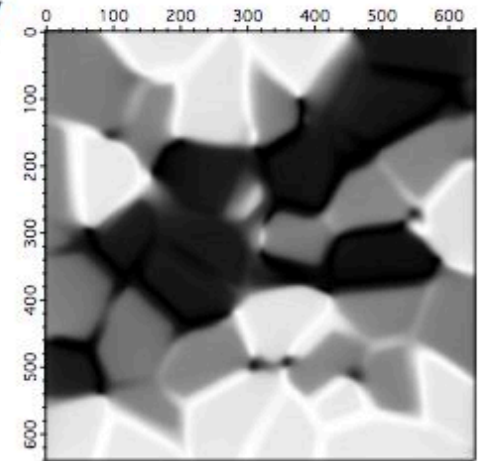
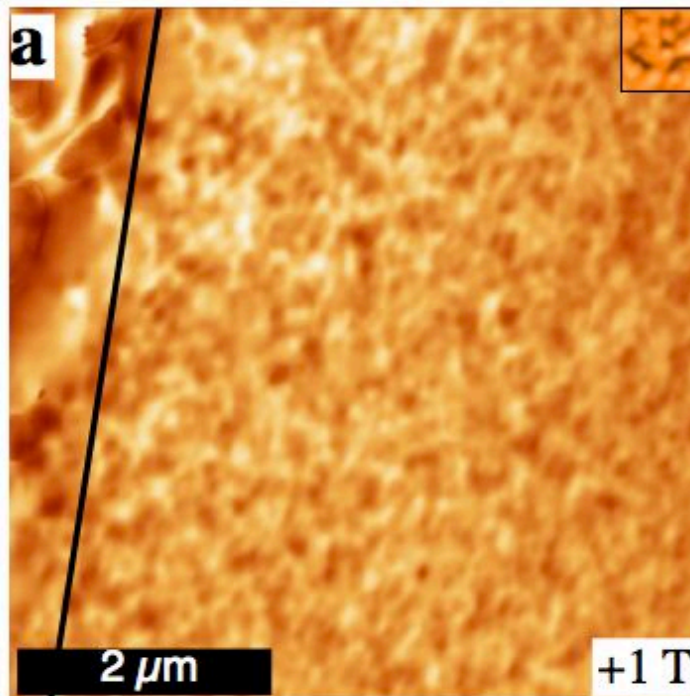
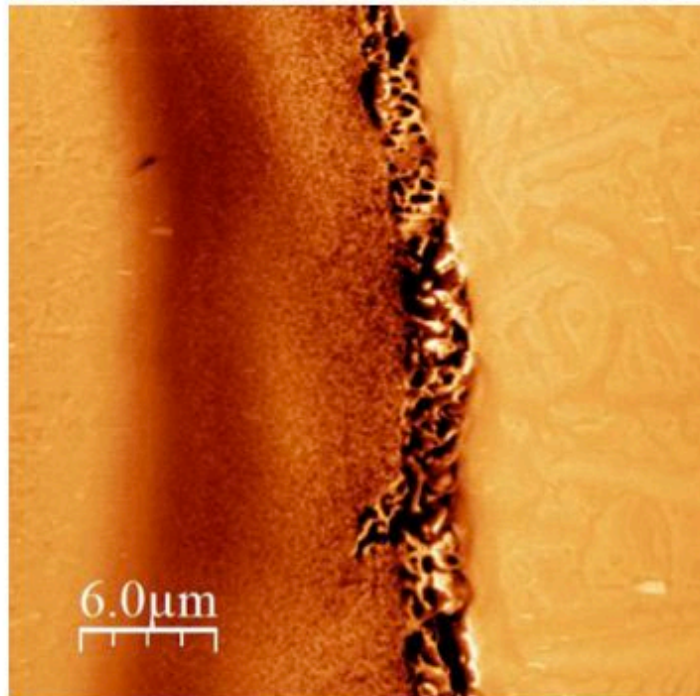
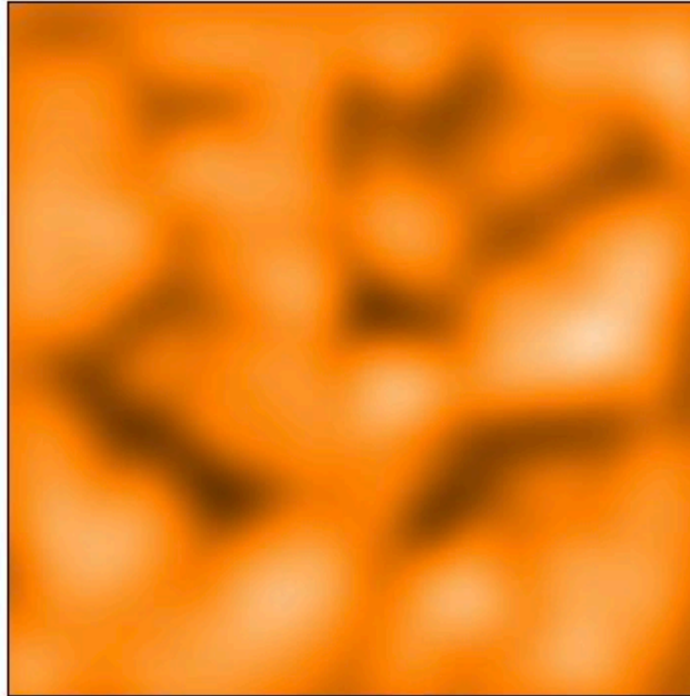
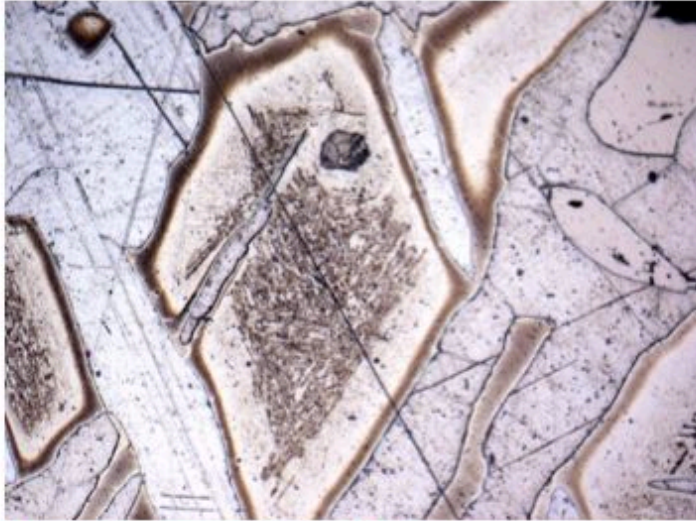
Micromagnetic simulation



1. 3D discretised model created of an island-matrix microstructure with length scales matching those observed experimentally.
2. Each island assigned properties of FeNi (ferromagnetic, high anisotropy) with uniaxial easy axis direction along one of the three $\langle 100 \rangle$ directions of the host.
3. Matrix phase assigned properties of Fe_3Ni (ferromagnetic, zero anisotropy).
4. Islands and matrix exchange coupled across interface with average exchange constant for FeNi and Fe_3Ni .



Magnetic Force Microscopy

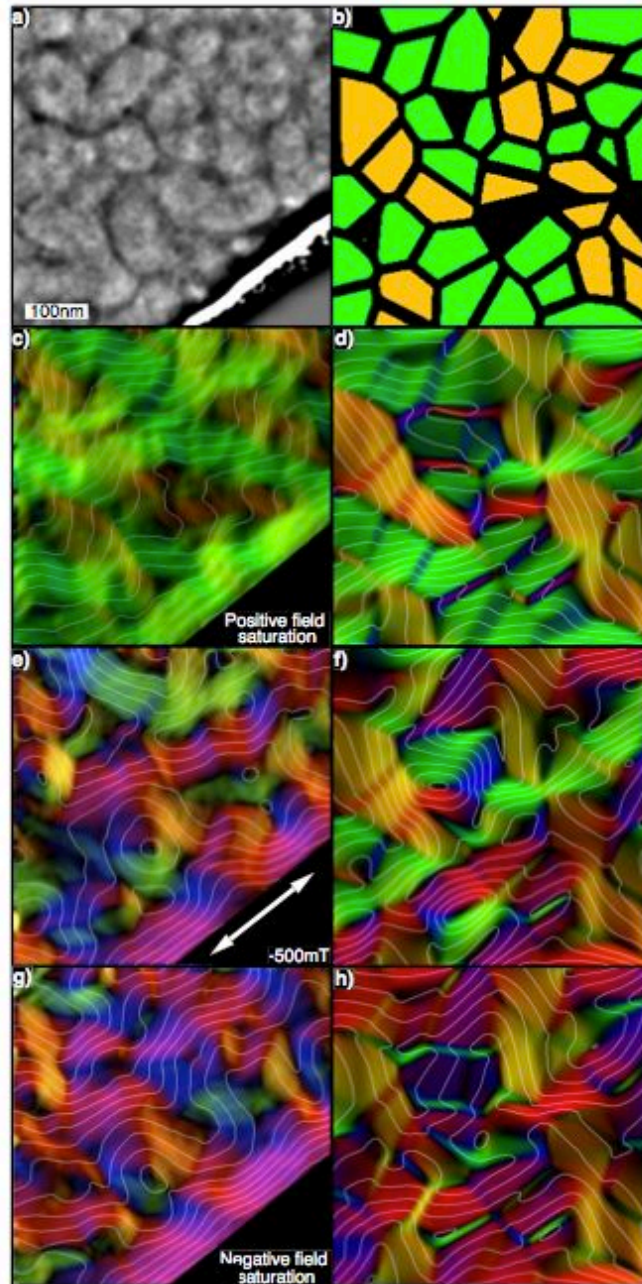


Electron Holography

Non-magnetic matrix

Exp

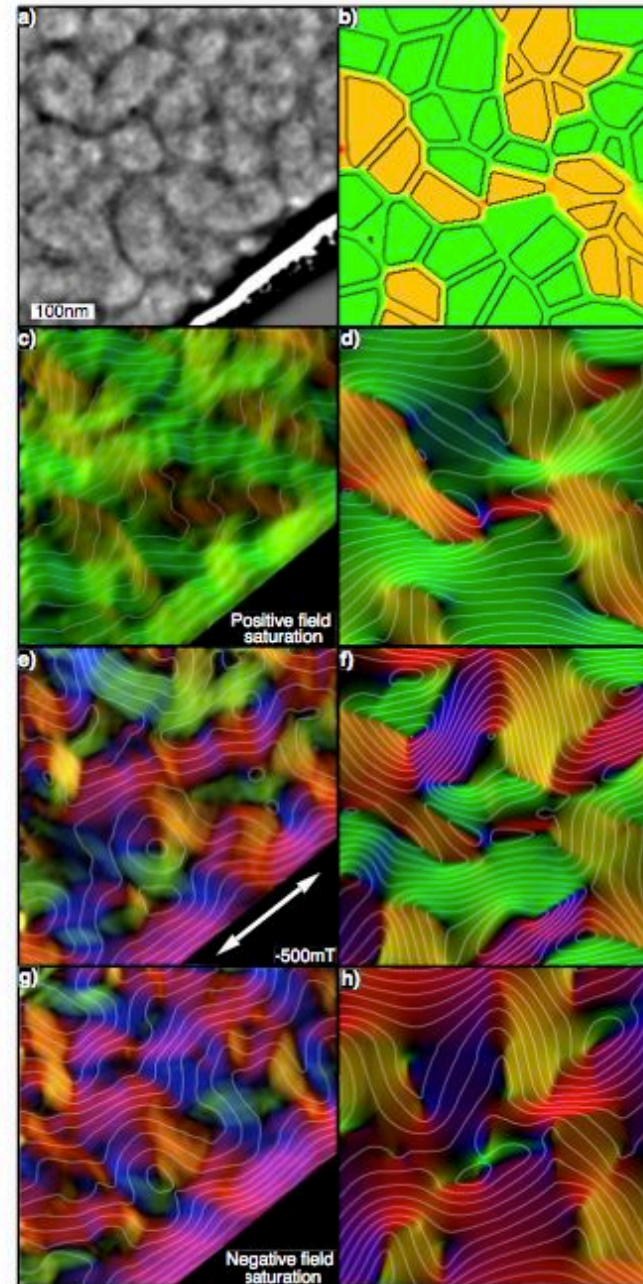
Sim



Magnetic matrix

Exp

Sim

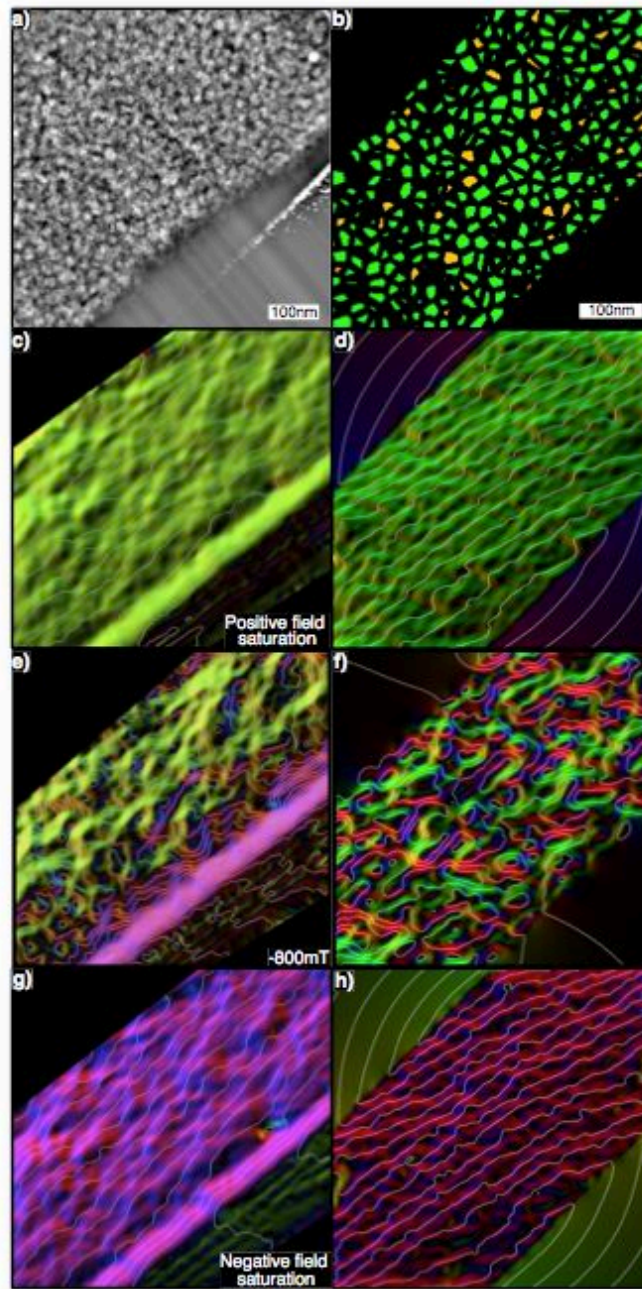


Electron Holography

Non-magnetic matrix

Exp

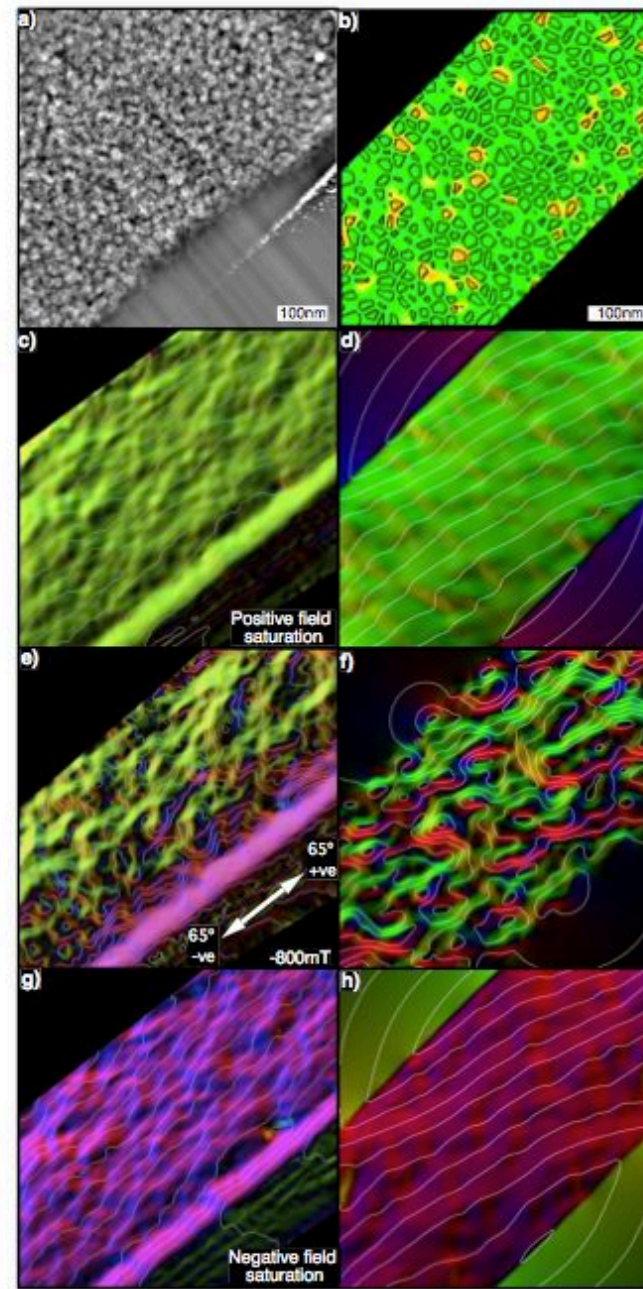
Sim



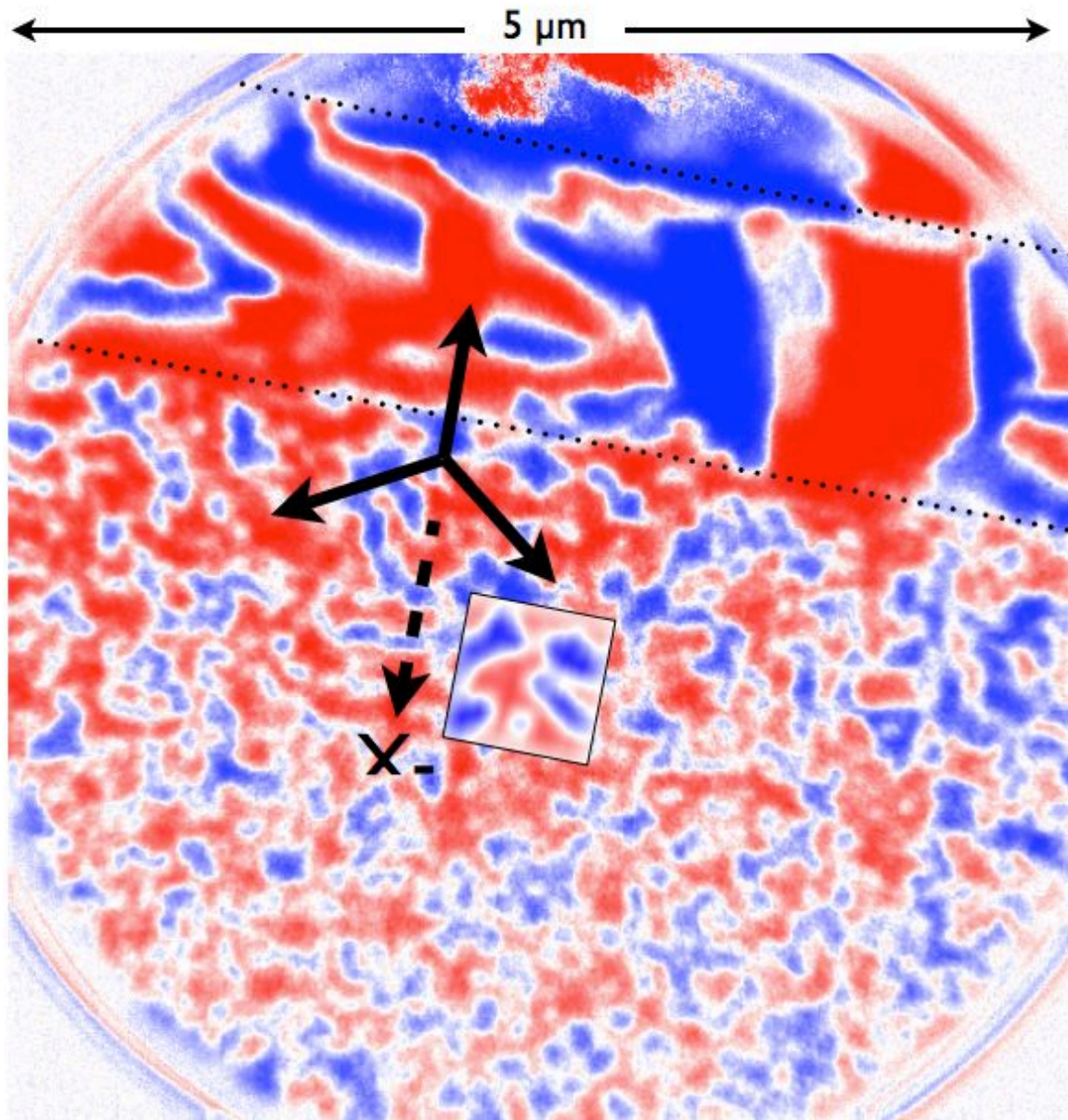
Magnetic matrix

Exp

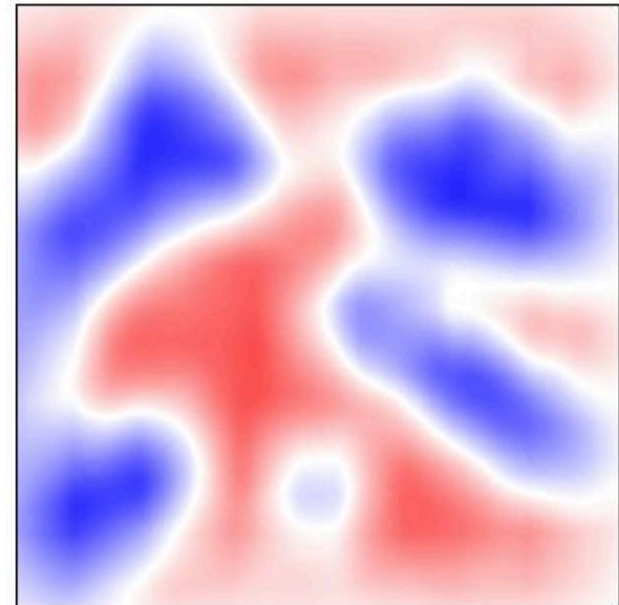
Sim



X-ray Photoemission Electron Microscopy (X-PEEM)

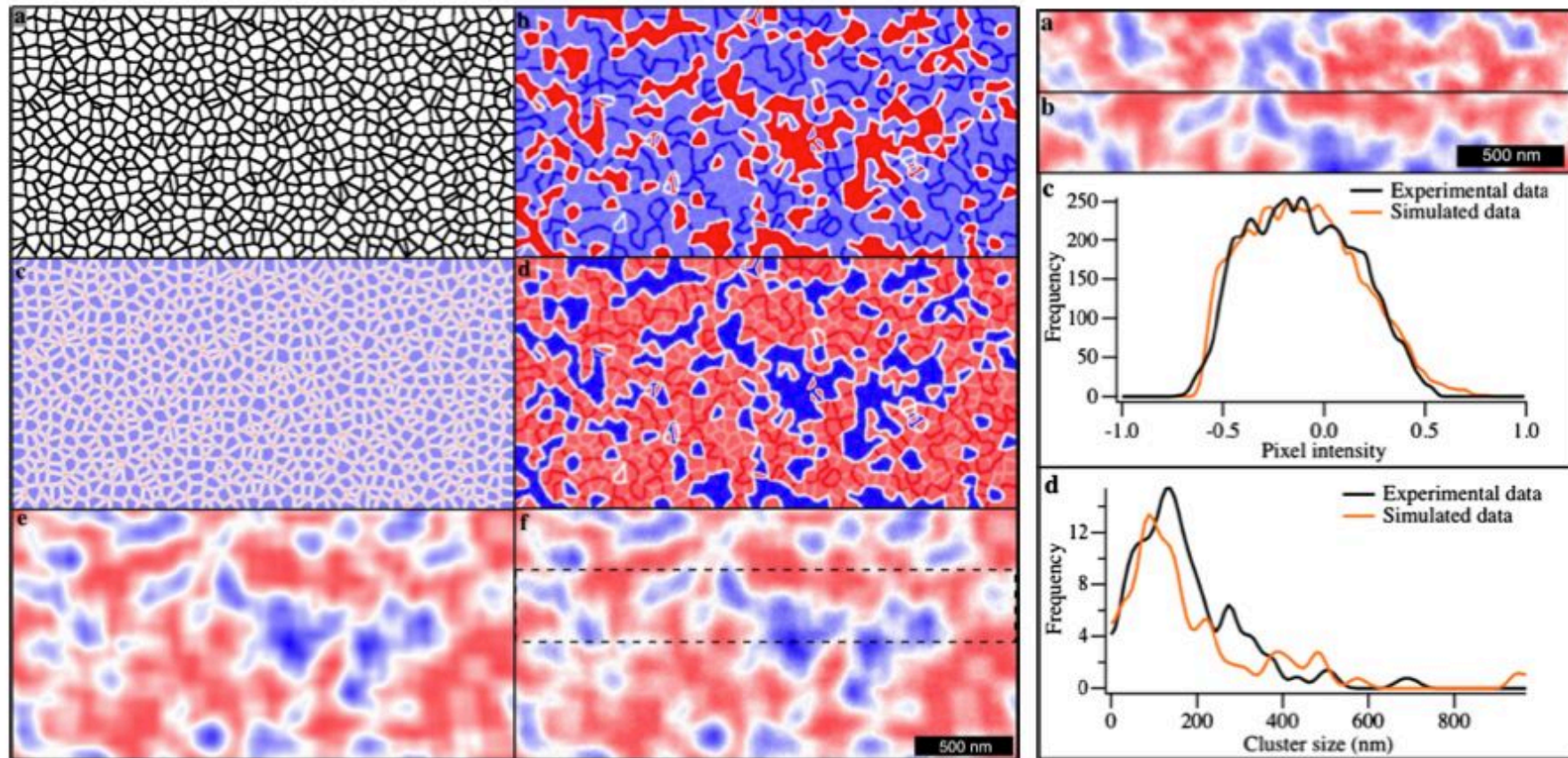


X-PEEM measures surface magnetisation directly. Simulating the image simply involves projecting the simulated magnetisation onto the X-ray direction and convoluting with experimental resolution function ($\sim 120\ \text{nm}$ in this case).



X-ray Photoemission Electron Microscopy (X-PEEM)

Once the micromagnetic principles are understood, we can take the simulation further using simplified computer generated magnetisation models. Comparison of the pixel intensity histograms allows quantitative nanopaleomagnetic directions and intensities to be extracted from the cloudy zone.



DEMO

Magnetic Microscopy: seeing is believing

Part I

- Overview of magnetic microscopy methods
- Why the need for forward modelling?
- ATHLETICS
- Theory
- Examples

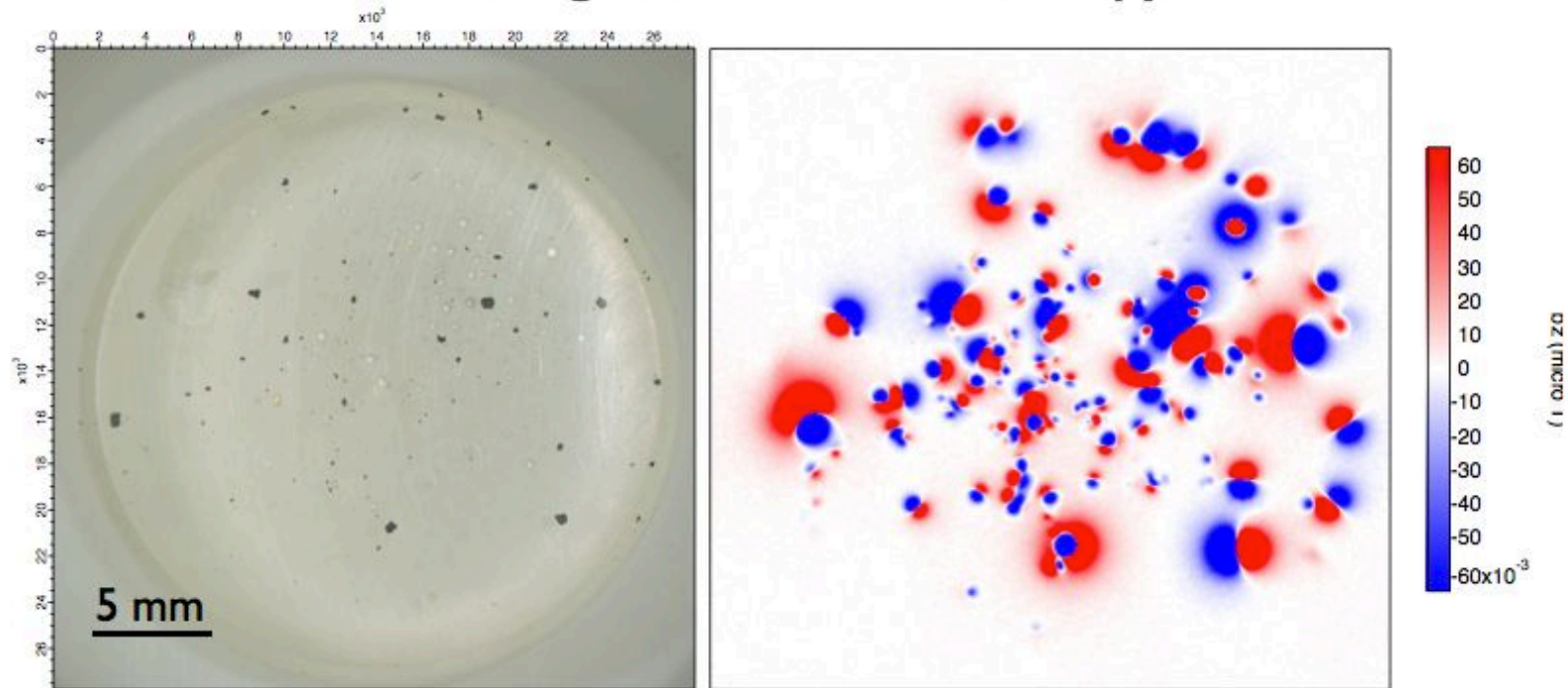
Part II

- Demonstration of ATHLETICS in action

Overview of magnetic microscopy methods

Modern magnetic microscopy methods cover a wide range of length scales (and time scales) of interest to rock magnetism.

Scanning SQUID microscopy

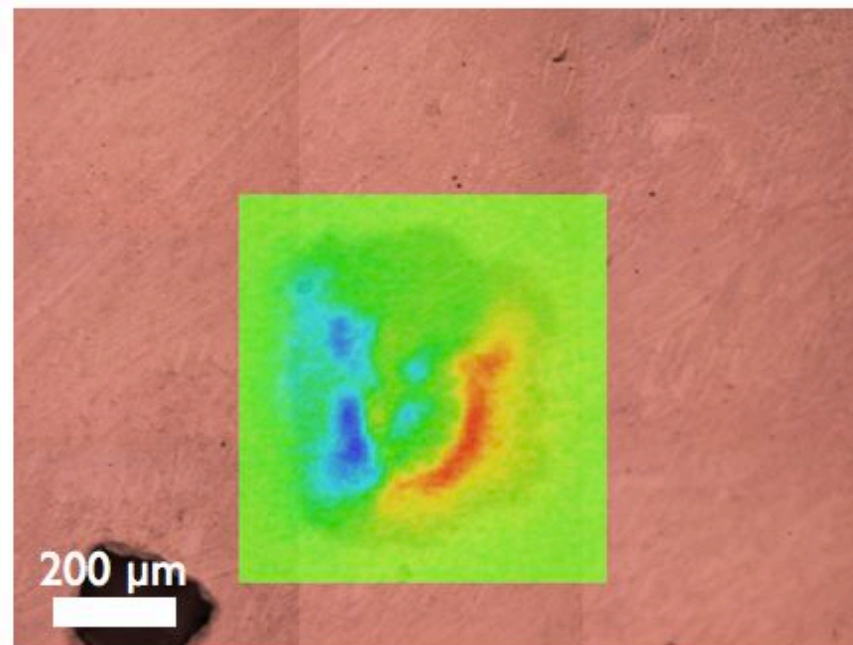


Resolution $\sim 100 \mu\text{m}$
Field-of-view $\sim \text{cm}$
Measurement time $\sim \text{hours}$
Measures: stray field

Overview of magnetic microscopy methods

Modern magnetic microscopy methods cover a wide range of length scales (and time scales) of interest to rock magnetism.

Scanning MTJ microscopy



Resolution $\sim 10 \mu\text{m}$

Field-of-view $\sim \text{mm}$

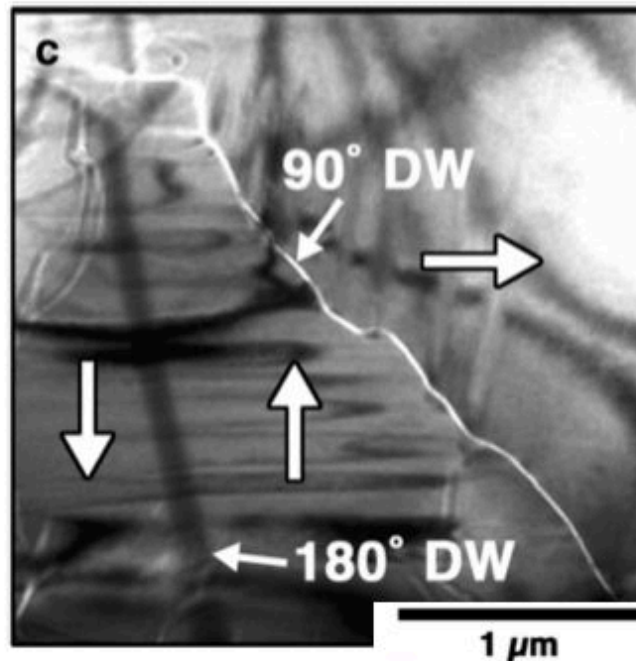
Measurement time $\sim \text{minutes}$

Measures: stray field

Overview of magnetic microscopy methods

Modern magnetic microscopy methods cover a wide range of length scales (and time scales) of interest to rock magnetism.

Lorentz microscopy



Resolution ~100 nm

Field-of-view ~10-100 μm

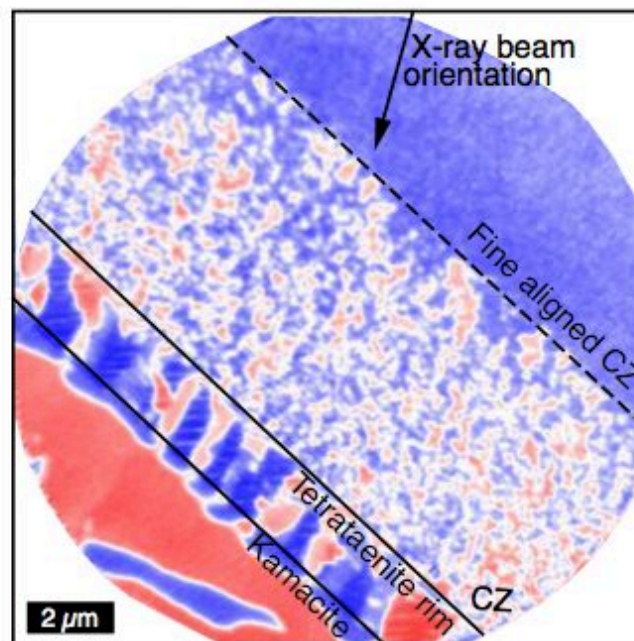
Measurement time ~seconds

Measures: second derivative of electron phase shift

Overview of magnetic microscopy methods

Modern magnetic microscopy methods cover a wide range of length scales (and time scales) of interest to rock magnetism.

X-ray Photo Emission Electron Microscopy (X-PEEM)



Resolution ~30 nm

Field-of-view ~5-20 μm

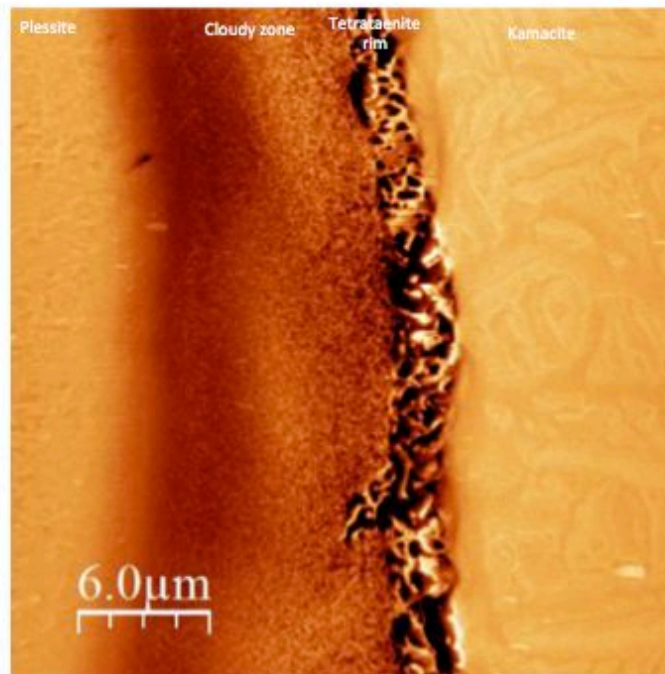
Measurement time ~minutes (but with potential for pico second resolution)

Measures: surface in-plane magnetic moment (projected along X-ray direction)

Overview of magnetic microscopy methods

Modern magnetic microscopy methods cover a wide range of length scales (and time scales) of interest to rock magnetism.

Magnetic Force Microscopy (MFM)



Resolution ~10s of nm

Field-of-view ~10-100 μm

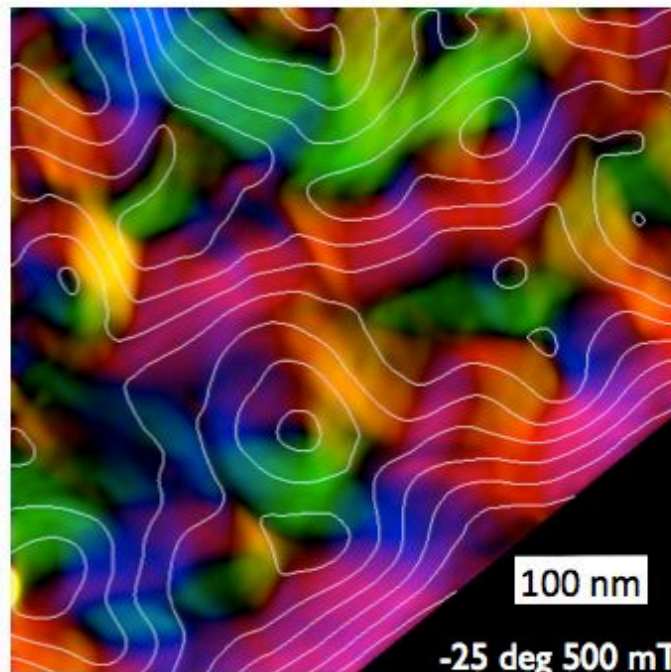
Measurement time ~minutes-hours

Measures: second derivative of stray field

Overview of magnetic microscopy methods

Modern magnetic microscopy methods cover a wide range of length scales (and time scales) of interest to rock magnetism.

Electron Holography



Resolution ~ 1 nm

Field-of-view ~ 1 μm

Measurement time \sim minutes

Measures: electron phase shift (integrated magnetic induction)